ES Energy & Environment

REVIEW PAPER View Article Online

Recent Advance on Graphene in Heat Transfer Enhancement of Composites

Changqing Liu[1,2], Mao Chen[1,2], Wei Yu[3*] and Yan He[4*]

Graphene, a monolayer of carbon atoms arranged in hexagonal honeycomb lattice with sp^2-hybridized orbital, exhibits large specific surface area and super high thermal conductivity. Therefore, graphene-based polymer composites have great potential in the field of thermal management, such as nanofluids, thermal conductive polymer materials, thermal interface materials and phase change materials. In this review, firstly, the intrinsic thermal conductivity of graphene is introduced, and it is mainly affected by edge conditions, size, defects and hydrogen functionalization. Secondly, the application of graphene in improving thermal transport properties of composites is presented. Lastly, the factors affecting the thermal transport properties of composites and the common improvement methods are summarized systematically. These methods include directional alignment, functionalization and synergistic enhancement. We believe these recent advances will provide useful reference for researchers.

Keywords: Graphene; Heat transfer; Nanofluids; Polymer composites; Phase change materials

Received 29 November 2018**, Accepted** 5 December 2018

DOI: 10.30919/esee8c191

Introduction

Graphene is the most typical two-dimensional material, consisting of a monolayer of carbon atoms arranged in hexagonal honeycomb lattice with sp^2-hybridized orbital. Currently, the kinds of prepared graphene mainly including single-layer graphene, few-layer graphene and three-dimensional graphene foam , exhibits many excellent characteristics due to unique structure, such as superstrength, ultrafast carrier transport capacity, super high thermal conductivity and extremely low light absorptivity.[1-4] Due to these advantages, graphene is widely used in sensors, flexible displays, new energy batteries, hydrogen storage materials, aerospace, composite materials and other fields.[5-12]

High intrinsic thermal conductivity is an important characteristic for graphene, which attracts extensive research interests in the field of thermal science. It is mainly used to enhance the thermal transport properties of thermal functional composites such as nanofluids, thermal conductive polymer materials (TCP), phase change materials (PCMs) and thermal interface materials (TIMs). Furthermore, it is agreed that interface thermal resistance is a key factor for the thermal transport properties of graphene-based thermal functional composites. So far, many methods such as directional alignment, functionalization, synergistic effect and three-dimensional graphene have been used to reduce the interface thermal resistance.[13-15] Although the thermal properties of graphene-based composites have been improved to some extent, the effect is not very significant, and the mechanism of heat transfer enhancement is not clear.

In this brief comment, the thermal properties of graphene and graphene film are summarized. Moreover, the current problems, possible solutions and future directions for graphene in heat transfer enhancement of composites are systematically reviewed. The composites include nanofluids, thermal conductive polymer materials, thermal interface materials and organic phase change materials (Fig. 1).

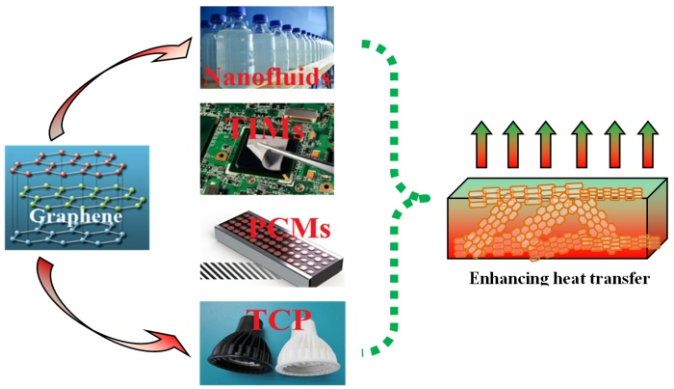

Fig. 1 Applications of graphene in heat transfer enhancement of composites.

[1]*School of Mechanical and Energy Engineering, Shaoyang University, Shaoyang, 422001, China*
[2]*Key Laboratory of Hunan Province for Efficient Power System and Intelligent Manufacturing, Shaoyang University, Shaoyang, 422001, China*
[3]*College of Engineering, Shanghai Polytechnic University, Shanghai, 201209, China*
[4]*School of Mechanical and Electrical Engineering, Qingdao University of Science and Technology, Qingdao, 266061, China*
***E-mail**: heyan_sd@163.com; E-mail: yuwei@sspu.edu.cn*

Thermal conductivity of graphene

Theoretical calculation prediction and experimental results all agree that graphene shows very high thermal conductivity. However, the edge conditions, defects and hydrogen functionalization will definitely affect the thermal transport properties of graphene based on theoretical calculation (see table 1).[16-22] Aksamija *et al.*[16] found that the highest thermal conductivity occurred in the zig-zag direction and the lowest in armchair graphene nanoribbons (GNRs) by molecular dynamics simulations. In addition, narrow GNRs with rough edges must show the smallest and most anisotropic thermal conductivity. Guo *et al.*[17] have studied the effect of edge shapes on the thermal conductivity of GNRs, such as different width, length and strain (Figs. 2a 2b). It was found the thermal conductivity was very sensitive to the edge shapes. Moreover, the thermal conductivity of armchair GNRs monotonously increased with width, while the thermal conductivity of zig-zag GNRs first increased and then decreased with the increasing width. Evans *et al.*[18] have computed the thermal conductivity of GNRs with rough and smooth edges (Fig. 2c). The results indicated that the highest thermal conductivity occurred in smooth edge whether it is zigzag or armchair edges. Due to the important effect of phonon scattering in the edge, the thermal conductivity depended strongly on the width of GNRs with rough edges.

The influence of defects on the heat transfer properties of graphene were investigated by using molecular dynamics simulations, including Stone–Thrower–Wales dislocations and monatomic vacancies (Fig. 2d).[19] It was indicated that the thermal conductivity of graphene sheet with defect showed a strong dependence on the number of defects. Moreover, propagating mode was translated into diffusive mode with increasing number of defects, as a result of the scattering of phonons in defects position and delocalized interaction between phonons. Ng *et al.*[20] investigated the effect of concentration of Stone–Thrower–Wales defects on the heat transfer properties of GNRs with zigzag or armchair edges. The results exhibited that the thermal conductivity will decrease by more than 50 % in virtue of the defect. Furthermore, the thermal conductivity of GNRs monotonously decreased with defect density, significantly higher in zigzag than in armchair GNRs at all concentration of defect.

The role of hydrogen functionalized on the heat transfer properties of graphene with armchair was investigated by nonequilibrium molecular dynamics simulation. The thermal conductivity showed a

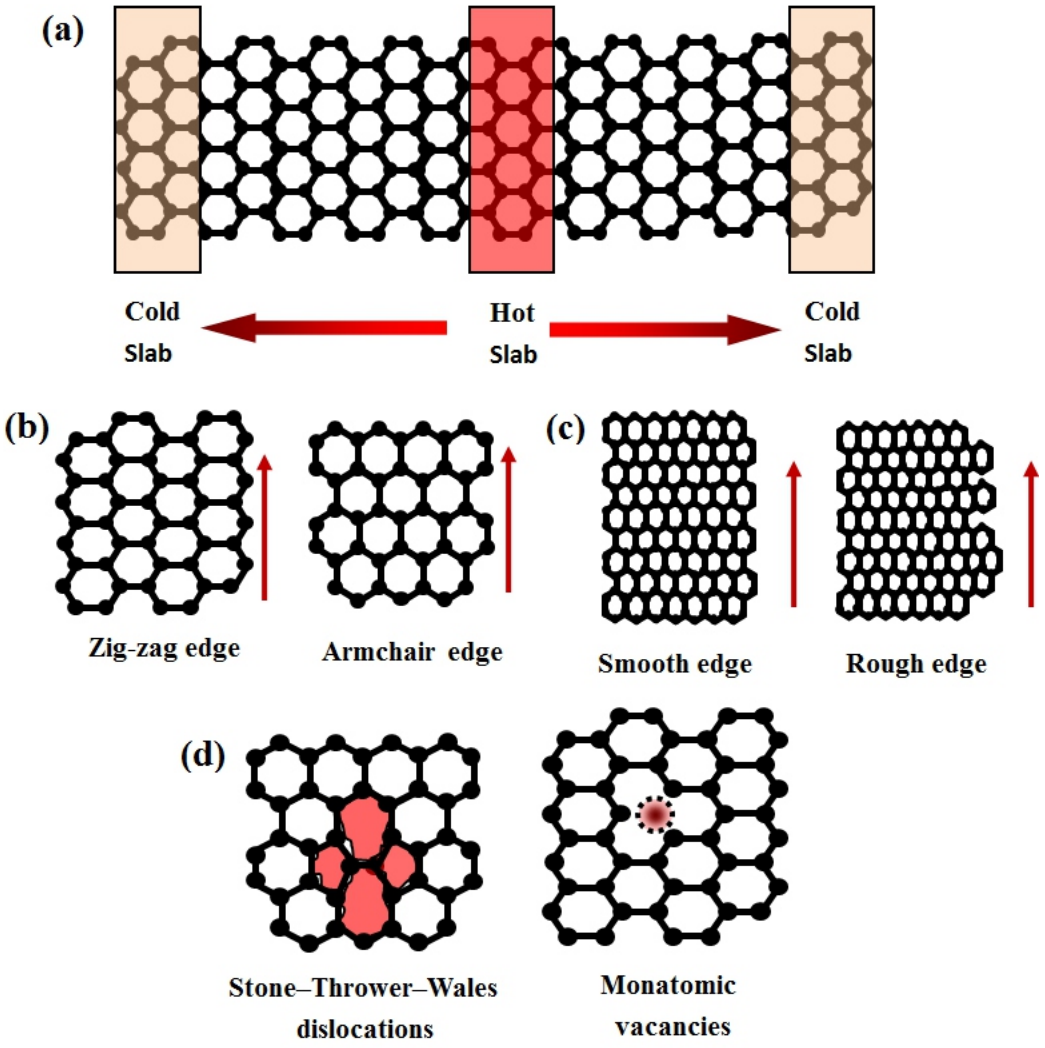

Fig. 2 Relevant descriptions for calculating the thermal conductivity of graphene: (a) Schematic for reverse non-equilibrium molecular dynamics; (b) Zig-zag edge and armchair edge; (c) Smooth edge and rough edge; (d) Stone–Thrower–Wales dislocations and monatomic vacancies.

Table 1 Comparing the thermal conductivity of graphene from different conditions based on theoretical calculation.

Sample	Temperature	Size	Edge and defect	Thermal conductivity ($Wm^{-1} K^{-1}$)	Calculation method	Reference
Graphene nanoribbons	100 K	width 1 μm	zig-zag edge	4700~5200	first-principles numerical calculations	16
Graphene nanoribbons	290 K ~310 K	length 11 nm	zig-zag edge (10-80 layers)	480~520	nonequilibrium molecular dynamics	17
Graphene nanoribbons	300 K	width 2 nm ~ 12 nm	smooth zigzag edge	3000~7000	nonequilibrium molecular dynamics	18
Graphene nanoribbons	300 K	width 2.1 nm length 10.0 nm	zigzag edge, number of defects (2-10)	40~80	molecular dynamics	19
Graphene	300 K	length (6 nm) width (about 2.5 nm)	armchair edge functionalized with hydrogen (10 %~50 %)	50 ~60	nonequilibrium molecular dynamics	21

rapid drop for graphene with hydrogen coverage. Moreover, it was reduced by about 40 % when hydrogen coverage accounted for only 2.5 % of the total number of carbon atoms.[21] Evans *et al.*[14] also found that hydrogen termination significantly dropped the thermal conductivity of graphene, which was attributed to phonon scattering from the edge.

How to accurately measure the thermal conductivity of graphene is still a great challenge. Conventional measurement methods are no longer suitable due to scale effect. However, many new methods have been developed, such as Raman optothermal technique (Fig. 3a),[23] steady state self heating method (Fig. 3b),[24] heat spreader method (Fig. 3c),[25] 3ω method[26] and other ways.[27-31] Furthermore, the measurement results of thermal conductivity vary greatly from different methods, because each method has its own unique application scope. The Raman optothermal technique is not suitable for the measurement of thermal conductivity of graphene with pollution, due to optical absorption loss.[32-34] The steady state self heating method is easy to measure the relationship between thermal conductivity and temperature. In addition, the heat spreader method is especially suitable for the measurement of thermal conductivity of graphene attached on the substrate.

The thermal conductivity of graphene is mainly affected by the number of atomic layer, length, temperature and isotopically modified in experimental results. Chen *et al.*[35] found that the thermal conductivity of isotopically pure ^{12}C (0.01% ^{13}C) graphene was higher than 4000 $Wm^{-1} K^{-1}$ at the measured temperature of 320 K, and twice as high as that composed of a 50:50 mixture of ^{12}C and ^{13}C (other data seen in Fig. 3e). Ghosh *et al.*[36] proved that the thermal conductivity varied from 2800 to 1300 $Wm^{-1} K^{-1}$ at room temperature as the number of atomic layers in few-layer graphene increased from 2 to 4 (Fig. 3f). Xu *et al.*[37] reported in experimental results that the thermal conductivity of suspended single-layer graphene increased with the length of the samples, and the function relation could be expressed as ~logL (fig. 3d). Xie *et al.*[23] measured the thermal conductivity of free-standing GNRs. It was observed that the thermal conductivity of GNRs was very sensitive to temperature. The values increased from 126.21 $Wm^{-1} K^{-1}$ to 877.32 $Wm^{-1} K^{-1}$ in the temperature range from -75 to 100 °C, especially with abruptly large value of 1044.41 $Wm^{-1} K^{-1}$ at 50 °C.

Heat transfer properties of graphene films

Graphene film with high thermal conductivity shows great advantages as flexible lateral heat spreaders for electronics.[38-43] Yu *et al.*[38] successfully fabricated flexible graphene oxide film (GO film), and investigated thermal transport properties. The results confirmed that the GO film exhibited significant anisotropic thermal conductivity (Fig. 4a). The thermal conductivity along in-plane direction was 1.68–2.21 $Wm^{-1}K^{-1}$ by transient electrothermal technique, and the thermal diffusivity was $1.32–1.57\times10^{-6}$ m^2/s. However, the thermal diffusivity along cross-plane direction was only 1.68×10^{-7} m^2/s, because the GO film was made of stacked graphene oxide, in which heat could easily be transferred along the in-plane direction, while vertical heat transfer had to flow through the micro interface between the layers. In order to reduce interfacial thermal resistance between the GO layers, Yu *et al.*[39] have successfully prepared alkaline earth metal ions (Mg^{2+} and Ca^{2+}) modified GO thin film. It showed the thermal conductivities of Mg^{2+}-GO film and Ca^{2+}-GO film were 32.05 $Wm^{-1}K^{-1}$ and 61.38 $Wm^{-1}K^{-1}$ (Fig. 4b), respectively, indicating remarkable improvement in thermal transport properties compared to pure GO film. This was attributed to the fact that alkaline earth metal ions act as crosslinking agents to connect adjacent graphene oxide nanosheets, and further make GO layers more orderly, thus reducing interfacial thermal resistance and increasing thermal conductivity. Song *et al.*[40] have fabricated reduced GO film by annealing. With the increase of heat treatment temperature, more oxygen containing functional groups in the GO were removed, as well as carbon atoms were conversed from sp^3 to sp^2. The reduced GO film achieved an ultrahigh thermal conductivity of 1043.5 $Wm^{-1}K^{-1}$ when the annealing temperature reached 1200 °C. Besides 1000 °C was a critical point for thermal conductivity to increase dramatically (Fig. 4c). Kumar *et al.*[41] obtained reduced large-area GO film using simple chemical reduction method under mild conditions. The maximum surface area was as high as 1600 μm^2. These reduced large-area GO film showed large thermal conductivity of 1390 ± 65 $Wm^{-1}K^{-1}$, which than that of conventional reduced small-area GO film (900 ± 45 $Wm^{-1}K^{-1}$). This was because there were fewer defects in reduced large-area GO film, large-area GO film where sp^2 structure was destroyed near the edge boundary.

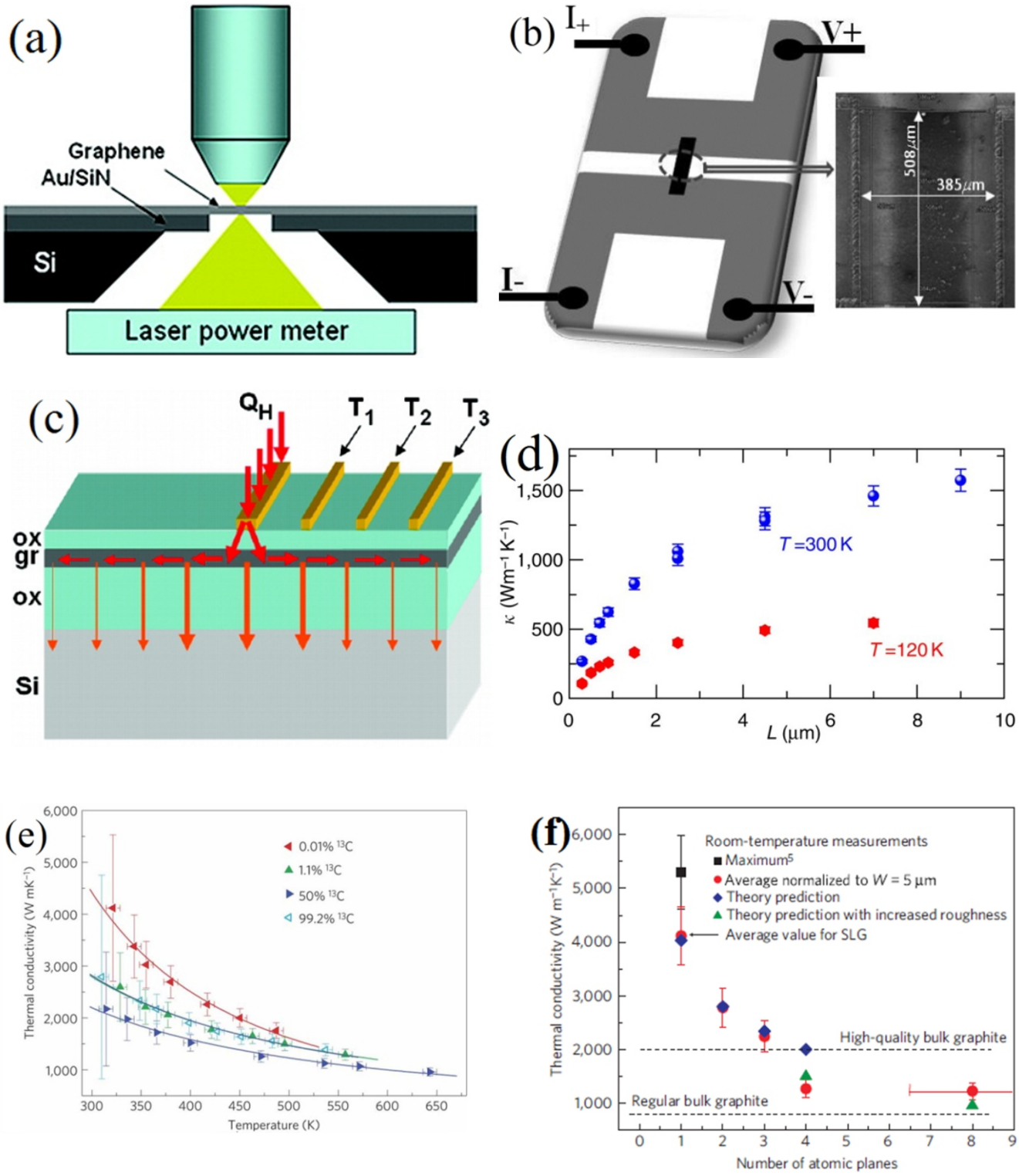

Fig. 3 (a) Schematic of the experimental setup for Raman optothermal technique; (b) Schematic diagram of the experimental setup for steady state self heating method; (c) Schematic of the heat spreader method; (d) Thermal conductivity of graphene versus sample length (L); (e) Thermal conductivity of the suspended graphene film with ^{13}C isotope concentrations of 0.01 %, 1.1 %, 50 % and 99.2 %, respectively, as a function of the temperature measured using the micro-Raman spectrometer; (f) Thermal conductivity of few-layer graphene as a function of the number of atomic planes. Reprinted with permission from Ref. 23, 24, 25, 35, 36 and 37.

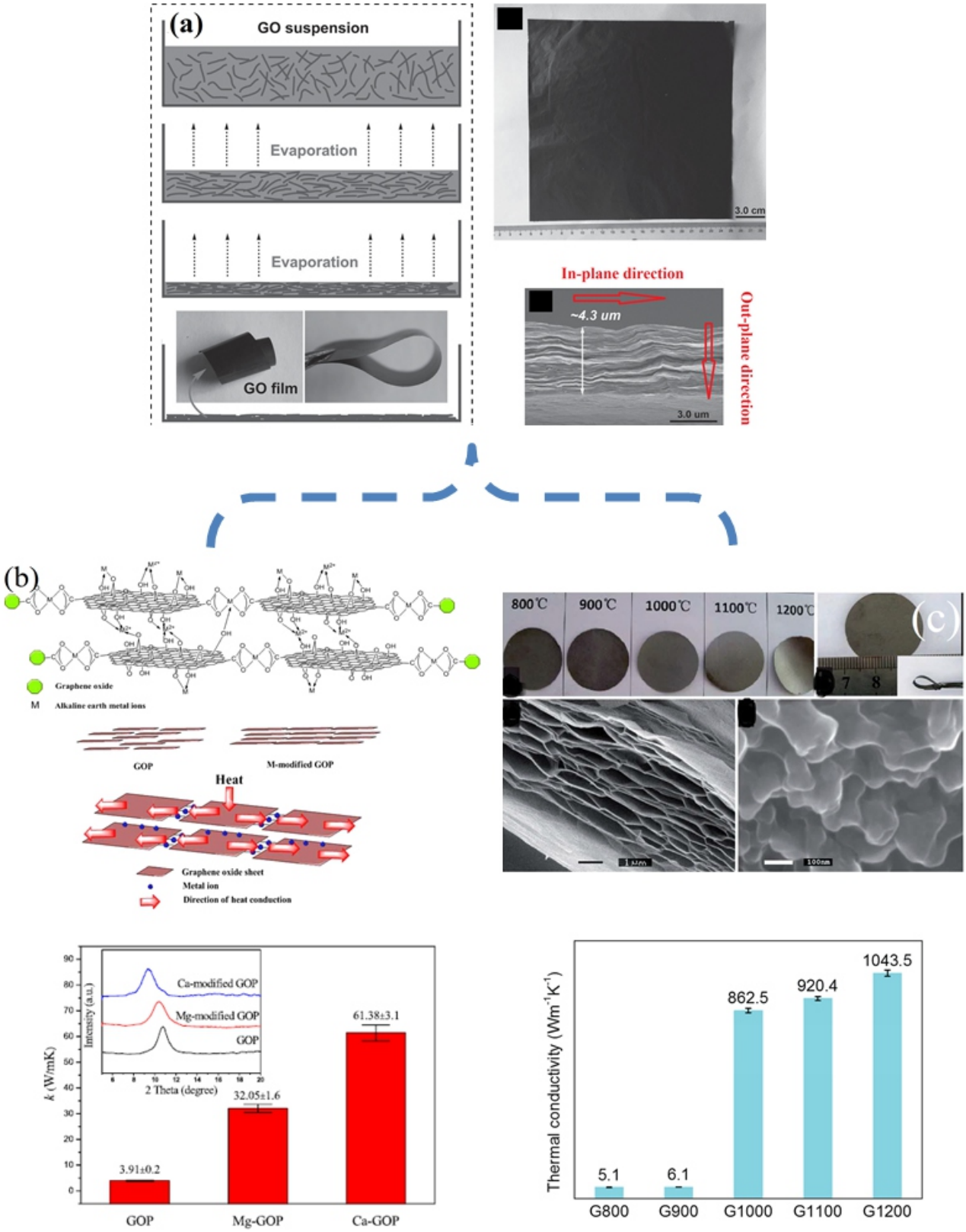

Fig. 4 (a) Layered GO film; (b) GO film modified with alkaline earth metal ions; (c) Reduced GO film fabricated by different annealing temperatures. Reprinted with permission from Ref. 38, 39 and 40.

The application of graphene in nanofluids

Nanofluids, composed of nanomaterials with high thermal conductivity and base fluid, are used in electronic equipment, nuclear energy, direct absorption solar thermal energy and heat pipe systems for enhancing forced convective heat transfer[44-45]. Types of base-fluid, types and shapes of particles and temperature are the three major factors affecting the convective heat transfer coefficient of nanofluids. Furthermore, the thermal transport properties of nanofluids are influenced by temperature, base-fluid, morphology and filling fraction of filler, clustering, acidity and additives.[46-47] Encouragingly, graphene possesses many advantages, such as higher thermal conductivity, larger surface area/volume ratio, high dispersion stability, easy preparation, lower erosion, corrosion and clogging. Therefore, it has become an excellent additive in nanofluids.[48-49]

Results from literatures exhibit that the thermal transport properties of graphene-based nanofluids are affected by temperature, size, filling fraction and so on. Esfahani *et al.*[50] prepared water-based nanofluids filled with graphene oxide at mass fraction of 0.01 wt.%, 0.05 wt.%, 0.1 wt.% and 0.5 wt.%, respectively. Results showed that the thermal conductivity of graphene oxide based water was governed mainly by particle-size distribution and viscosity. The water-based nanofluids filled with GO exhibited significantly improved thermal conductivity compared to pure water. However, there was an optimal concentration for thermal conductivity enhancement. The thermal conductivity was first improved with increasing filling fraction of GO. However, further increase of filling fraction of GO would accelerate the agglomeration and thus decrease the thermal conductivity. Graphene was prepared by hydrogen induced reduction and exfoliation of graphite oxide, and followed by dispersing in the base fluids.[51] It is clearly seen from the result that the thermal conductivity was enhanced with increasing filling fraction and temperature (Fig. 5a). The mechanism for the increase of thermal conductivity in nanofluid can be considered from the stochastic motion of nanoparticles. The great improvement in thermal conductivity with temperature enhancement resulted from violent Brownian-like motion at high temperature.

The thermal transport properties and dispersion stability of nanofluids may be further improved using surface functionalization (Fig. 5b).[52-53] The are many references, like graphene nanoplatelets that are functionalized with hexylamine and dispersed in diesel oil. These results exhibited that the thermal conductivity increased compared to the pure diesel oil at the same temperature for nanofluids with functionalized graphene at all filling fraction.[54] Yu *et al.*[55] developed a simple and novel method to fabricate graphene nanosheets (GNSs) based ethylene glycol. The ethanol solution of graphene oxide was mixed with sodium dodecylbenzebesuefonate, and reduced by hydrazine. The thermal conductivity of the graphene based ethylene glycol was increased significantly compared to pure ethylene glycol, up to 86 % enhancement for the base fluid with graphene dispersion at 5.0 vol % (Fig. 5c). In addition, SiO_2-coated graphene was fabricated from tetraethyl orthosilicate by using facile chemical liquid deposition way, and then a nanofluid of water based graphene was successfully produced using the SiO_2-coated graphene. These results showed the hydrophilicity of graphene by SiO_2-coated modification was significantly

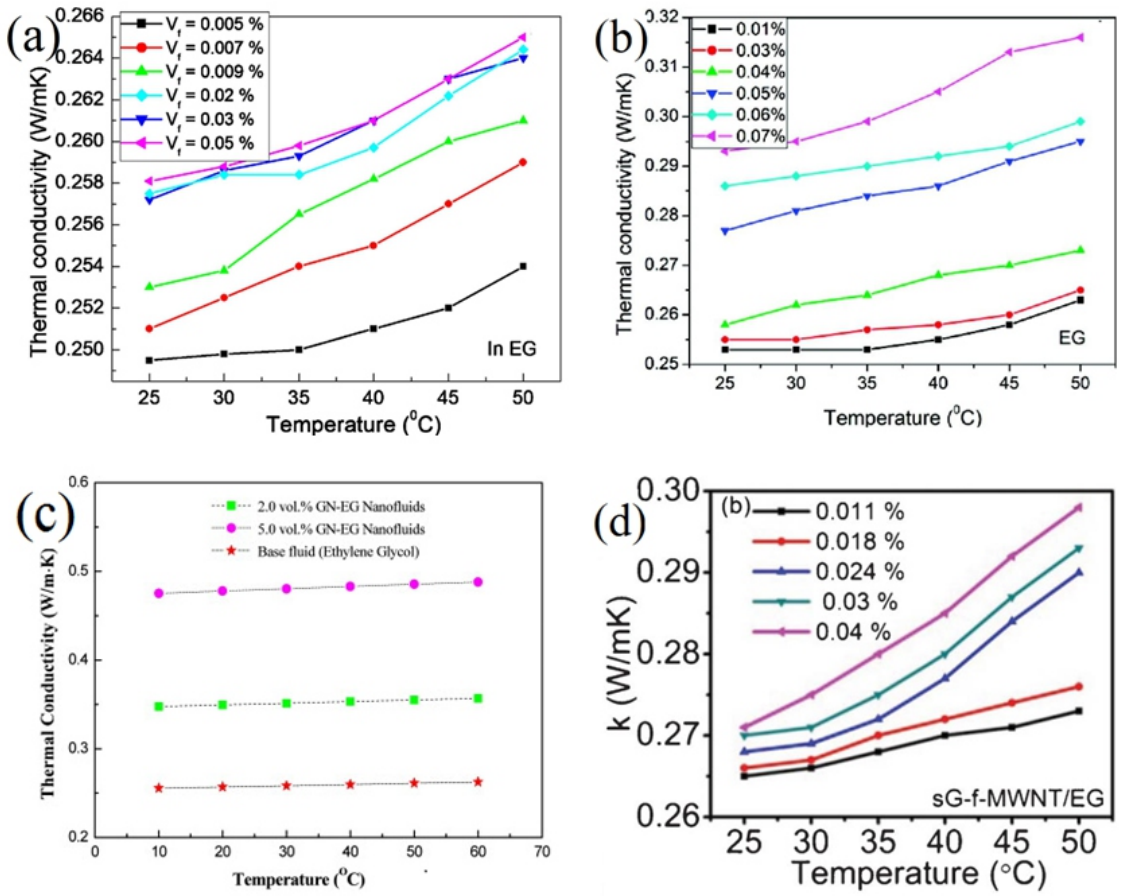

Fig. 5 Thermal conductivity of nanofluids with different volume fraction at varying temperature: (a) Functionalized graphene dispersed in ethylene glycol; (b) CuO modified graphene dispersed in ethylene glycol; (c) Graphene dispersed in ethylene glycol; (d) Graphene-MWNT dispersed in ethylene glycol. Reprinted with permission from Ref. 51, 52, 55 and 57

increased, while the dispersion stability and thermal transport properties of water-based nanofluid with SiO_2-coated graphene were also improved. Furthermore, it can enhance thermal conductivity superior to that water-based nanofluid with surfactants modified graphene.[56]

Aravind *et al.*[57] have studied the synergistic effect of graphene-MWNT nanocomposites on the thermophysical property of nanofluids. The thermal conductivity of de-ionized water with graphene and graphene-MWNT (0.04 % volume fraction) increased by 9.2 % and 10.5 % respectively at room temperature (Fig. 5d). The excellent thermal transport properties for nanofluid filled with graphene-MWNT composites could be attributed to high intrinsic thermal conductivity of graphene and MWNT, high aspect ratio, as well as unique complementary structure between graphene and MWNT.

Graphene has made some outstanding results in enhancing heat transfer of nanofluids. However, there are some problems that need to be solved: (1) further attention should be paid to the stability of nanofluids; (2) the standard of all experimental results is not uniform; (3) the mechanism for enhancement of heat transfer in nanofluids by graphene is still not clear.

Graphene in heat transfer enhancement for thermal interface materials

TIMs is filled between two rough solid contact surfaces (like heat source and radiator), eliminating the low thermal conductivity air and improving the thermal transport process. The total thermal resistance of heat transfer is composed of two contact thermal resistance and thermal resistance of TIMs. Therefore, excellent thermal transport properties and super wettability are the primary problems to be solved for TIMs.[58-60] So far, many types of TIMs have emerged, like particle-filled polymers, liquid metal and carbon materials based TIMs. Graphene-based TIMs have attracted great interest because graphene shows high thermal conductivity and large specific surface area.[61-62] Furthermore, interface thermal resistance is the key factor affecting the thermophysical properties of graphene-based TIMs.[63-65] The common idea is to build a high thermal conductivity network chain and improve the coupling state between graphene and matrix. [66-67]

The technology of directional alignment can achieve the "end to end" link of randomly dispersed graphene, and construct the heat conducting network chain in matrix (Fig. 6a). Yan *et al.* obtained highly aligned GNSs from magnetic GNSs–Fe_3O_4 in epoxy matrix by using magnetic field induced orientational ordering. GNSs–Fe_3O_4 was prepared by a simple coprecipitation method. The resulting GNSs–Fe_3O_4/epoxy composites showed high thermal conductivity in a parallel aligned GNSs direction at low loadings, far beyond the composites filled with randomly dispersed GNSs (Fig. 6c).[68] Renteria *et al.* studied the thermal transport properties of TIMs filled with magnetic field induced aligned graphene. Graphene was fabricated by using a low-cost and large-scale liquid-phase exfoliation. Moreover, magnetic Fe_3O_4 nanoparticles attached on the surface of graphene resulted in align the fillers under an external magnetic field during dispersion process. The thermal conductivity enhancement with the oriented GNSs–Fe_3O_4 hybrids was higher than that with the randomly dispersed fillers at low mass fraction (~1 wt %) by a factor of two times.[69]

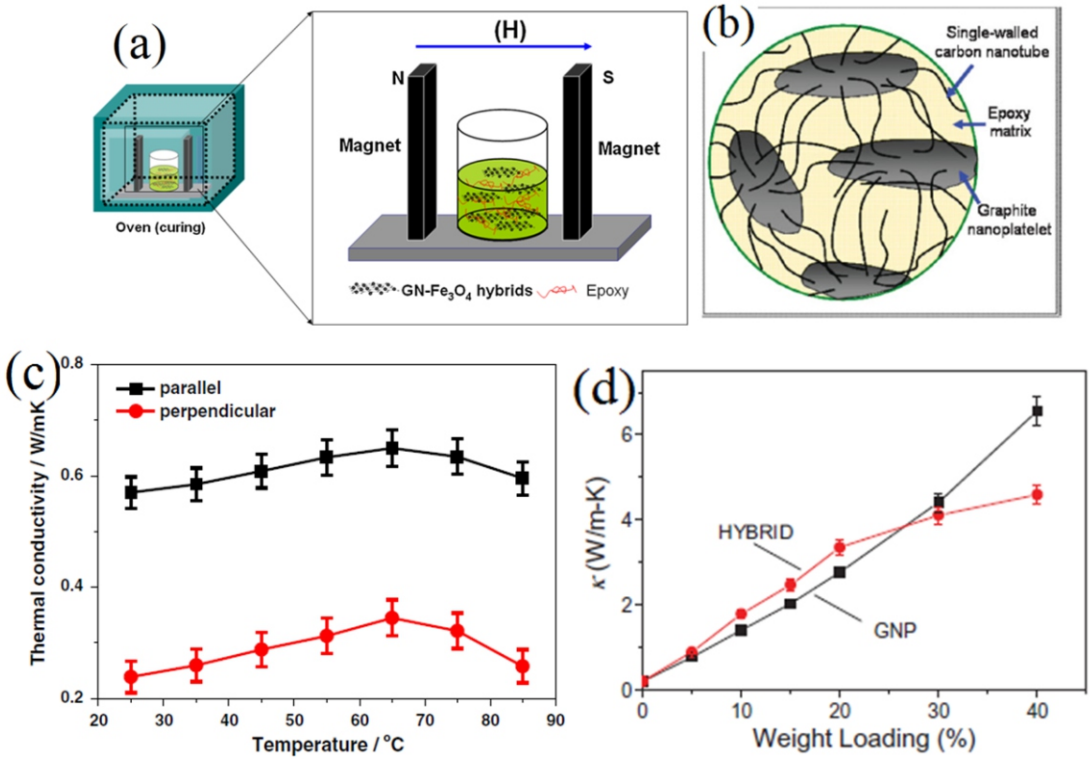

Fig. 6 (a) Schematic for the fabrication of GNSs–Fe_3O_4/epoxy composites by magnetic alignment; (b) Schematic of GNSs-SWNT network dispersed in polymer matrix; (c) The thermal conductivity of GNSs–Fe_3O_4/epoxy composites varying with temperature in parallel or perpendicular magnetic-alignment direction; (d) Thermal conductivity of GNSs-SWNT/epoxy (GNSs : SWNT=3 : 1) and GNSs/epoxy increase with the mass fraction of filler increase. Reprinted with permission from Ref. 68 and 74

Functionalization treatment can enhance the bonding between filler and matrix, and it can effectively reduce the interface thermal resistance. GNSs were functionalized through π–π stacking of pyrene molecules (Py-PGMA) with a functional segmented polymer chain. The Py-PGMA linked to the surface of GNSs not only make filler be more uniform dispersion in the matrix but also strengthen the interaction between filler and matrix. As a result, the thermal conductivity of composites with Py-PGMA–GNSs showed a great enhancement and was far beyond than that filled with pure GNSs. Furthermore, the thermal conductivity of composites filled with 4 phr Py-PGMA–GNS was increased by 20 % compared to that with pristine GNSs.[70] Based on molecular dynamics simulations, Wang *et al.* studied the influence of various covalently functionalized graphene on the interfacial thermal resistance between graphene and paraffin. The results exhibited that modifying graphene with functional group was a very effective method for reducing the interface thermal resistance. Furthermore, it depended mainly on the type and coverage of functional groups. However, there was a different conclusion on whether modification of graphene with functional groups could enhance thermal conductivity of composites.[71] Shen *et al.* demonstrated that modification of graphene with functional groups was effective in improving thermal property for small size of graphene, but invalid for large size of graphene.[72]

Remarkable synergistic enhancement of heat transfer was found between the two dimensional graphene and one dimensional carbon nanotubes (CNT), improving the thermal transport properties of epoxy based composites (Fig. 6b). CNT with the long and tortuous structure can connect adjacent GNSs and prevent their restacking, leading to a strong coupling state between the GNSs/CNT and the polymer matrix. Yang *et al.* studied the thermal property of CNT/GNSs/epoxy composites. When the mass fraction of filler was 1 %, the thermal conductivity of the composite exhibited a strong synergistic effect, and it was increased by 46.9 % compared to the pristine matrix.[73] Yu *et al.* also confirmed that there was synergistic enhancement of heat transfer between GNSs and CNTs. When the amount of GNSs/CNT mixture was 10 wt%, the thermal conductivity of composite was 1.75 Wm^{-1} K^{-1}, higher than the composite filled with only CNTs or GNSs (Fig. 6d).[74]

Graphene in heat transfer enhancement for thermal conductive polymer materials

Thermal conductive polymer composite is a promising functional material, which is attributed to excellent thermal transport property, corrosion resistance, easy processing and so on. It has a wide potential applications in the field of microelectronics, aerospace, military equipment, electronic and electrical appliances. Generally, the excellent thermal transport for filled high thermal conductive polymer composites depend largely on the performance of the filler. Graphene plays a very significant role in improving the properties of thermal conductivity polymer materials because of its ultrafast carrier mobility, super high thermal conductivity, large surface area and super strength.

Yu *et al.* prepared high thermal conductivity nylon-6 composites with GNSs as filler by mechanical blending.[75] The thermal conductivity of the composite increased linearly as the loading of GNSs increased. Furthermore, the thermal conductivity reached 4.11 Wm^{-1} K^{-1} at the volume fraction of 20 %, which was 15 times higher that compared to pure nylon-6. The result showed that the thermal transport property of particle-loading composite material was influenced by the type, particle size, structure, surface wetting and thermal conductivity of filler. Moreover, the graphene-based thermal conductive polymer with excellent thermal transport was mainly owing to graphene with high thermal conductivity, the low scattering of the phonon and transmission resistance. In addition, the two-dimensional plane structure with large surface area was easier to form a heat conduction network. GO sheets were modified with the assistance of polyvinylpyrrolidone using a simple non-covalent surface treatment method (Fig. 7a).[76] All the experimental results exhibited that modified GO can be dispersed homogeneously in the styrene–butadiene rubber matrix. With the presence of only 5 phr modified GO in the nano-composite, the thermal conductivity was increased by 30 % (Fig. 7b). Song *et al.* fabricated multilayered silicone rubber/graphene films with high thermal

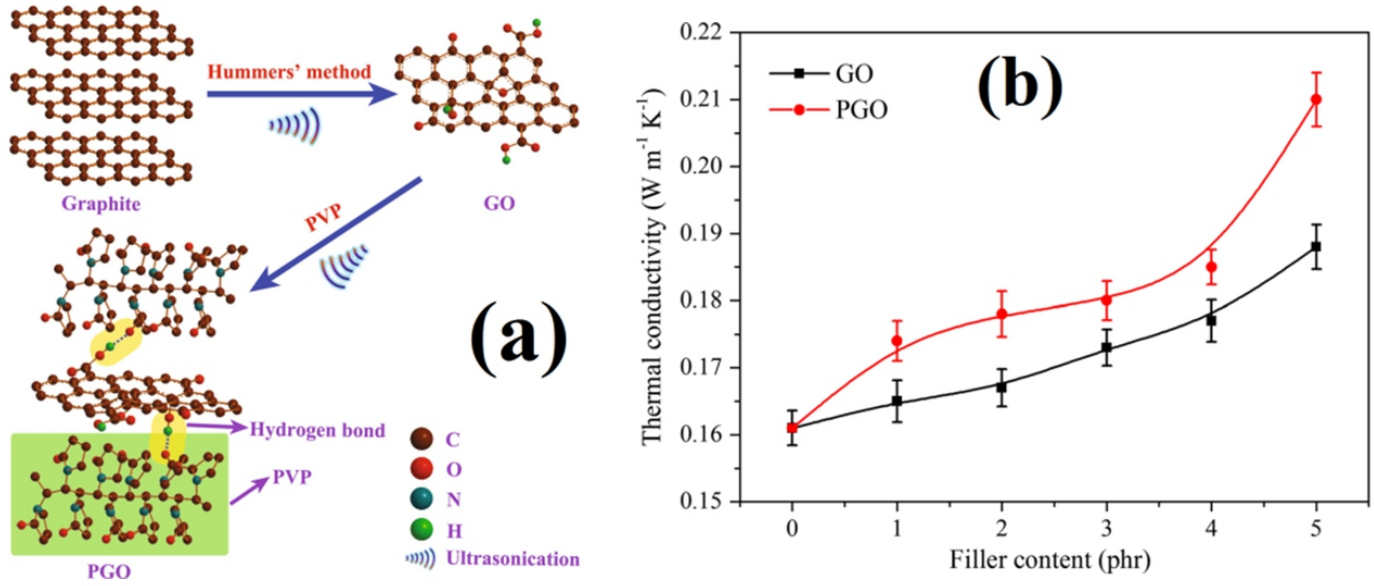

Fig. 7 (a) Schematic diagram for the formation of the hydrogen bonding between GO and polyvinylpyrrolidone (PVP); (b) Thermal conductivity for neat styrene–butadiene rubber (SBR), GO/SBR (Black solid line), and PVP-modified GO/SBR (Red solid line) composites. Reprinted with permission from Ref. 78.

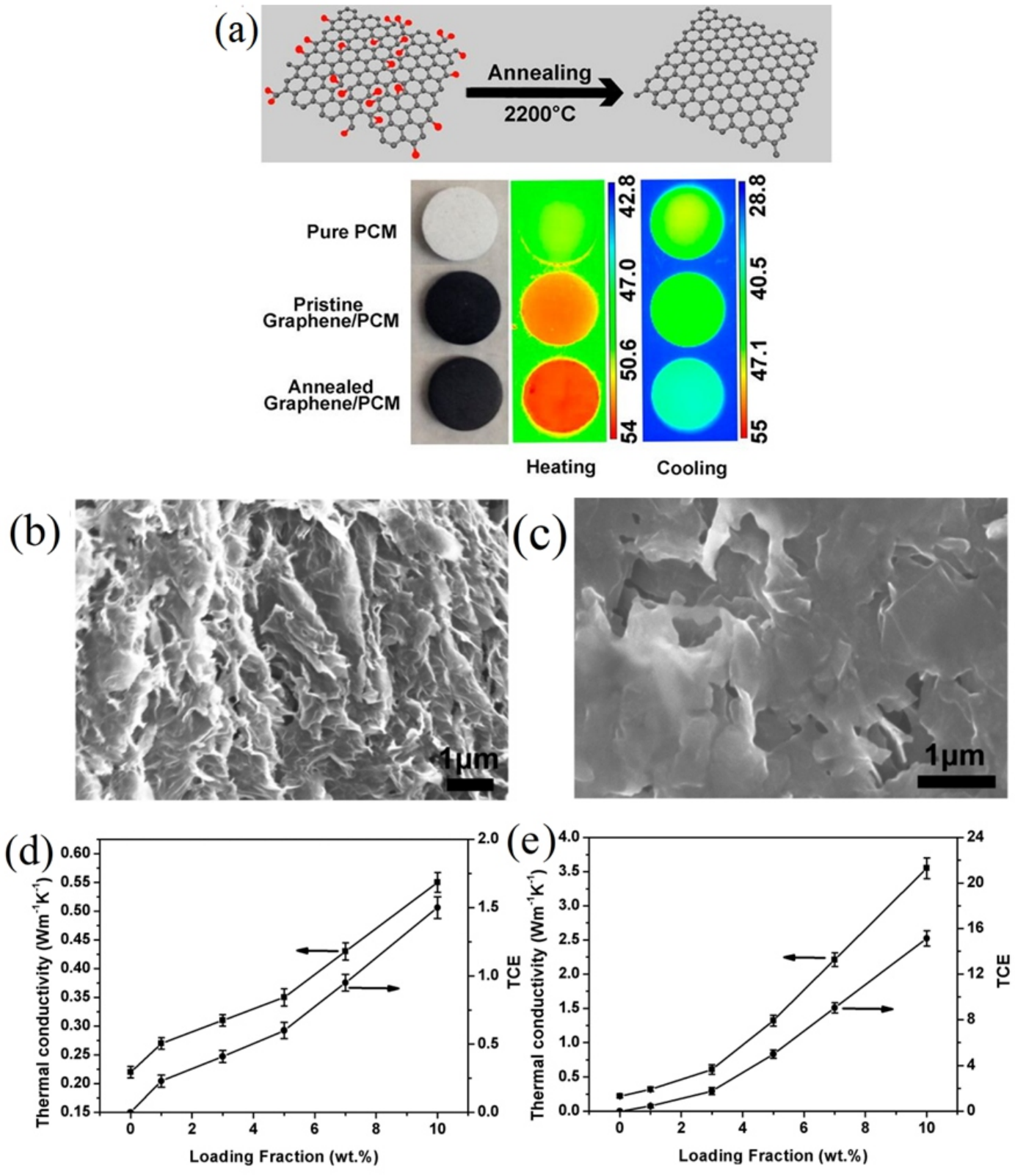

Fig. 8 (a) Infrared camera images of pure PCMs, pristine graphene PCMs and annealed graphene PCMs under heating or cooling; (b) (c)SEM images of pristine graphene PCMs and annealed graphene PCMs (10 wt% loading); (d) Thermal conductivity and enhancement percentage of PCMs filled with pure graphene at different loading; (e) Thermal conductivity and enhancement percentage of PCMs filled with annealed graphene at different loading. Reprinted with permission from Ref. 83.

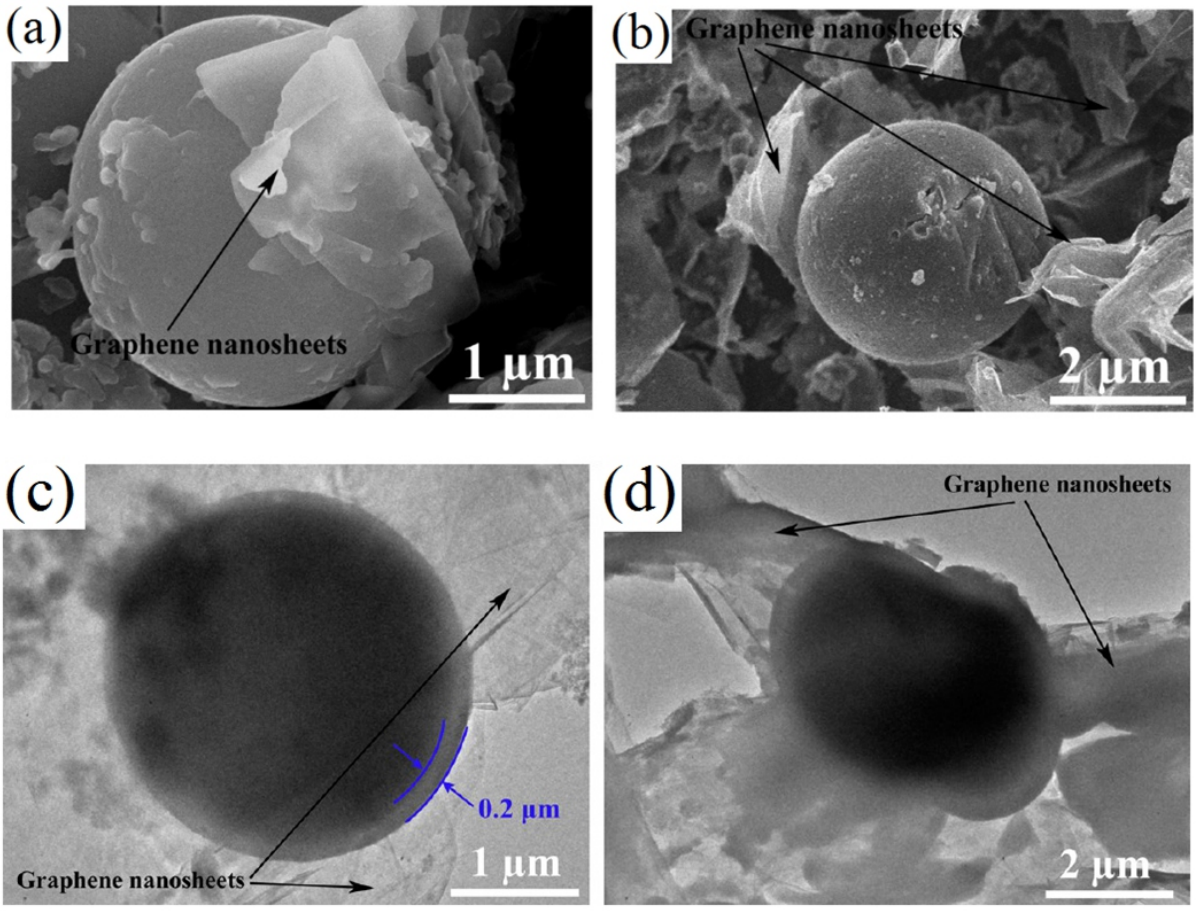

Fig. 9 SEM micrographs of n-eicosane@TiO_2@graphene microcapsules (a) 3 wt% graphene; (b) 5wt% graphene; TEM micrographs of n-eicosane@TiO_2@graphene microcapsules (c) 3 wt% graphene; (d) 5wt% graphene. Reprinted with permission from Ref. 90.

conductivity using a simple spin-assisted layer-by-layer assembly approach.[77] The films showed highly ordered layered structure with the neatly arranged GNSs which constructed an efficient heat transfer channel. A multilayered film with 40 assembly cycles at 2.53 wt% graphene loading had the thermal conductivity of 2.03 Wm^{-1} K^{-1} in in-plane direction. Liu *et al.* prepared styrene-butadiene rubber based composites by filling with mesoporous silica@reduced GO.[78] The mesoporous silica@reduced GO with sandwich structure was composed of reduced GO (0.50 wt%) coated with mesoporous SiO_2. The mesoporous SiO_2 attached to the surface of reduced GO impeded the aggregation of reduced GO and enhanced the bonding strength between reduced GO and matrix. When the addition of mesoporous silica@reduced GO at 3 per hundred rubber, the thermal conductivity was as high as 0.424 Wm^{-1} K^{-1}, which was 83 % enhancement compared to the thermal conductivity of pure styrene-butadiene rubber (0.232 $Wm^{-1}K^{-1}$).

Two-dimensional materials (graphene) and one-dimensional materials, zero dimensional nanomaterials can synergistically enhance the heat transfer of the composite system.[79-80] Recent studies showed that graphene and spherical alumina have obvious synergistic effect in improving the thermal transport property of thermal conductive silicone grease. When the amount of graphene is less (<1 wt%), it confirms a significant synergistic heat transfer effect. Furthermore, the higher the content of alumina in the composite system, the more significant the synergistic effect is. Song *et al.* prepared a novel hybrid of polymer grafted-CNT @ reduced GO by reversible addition-fragmentation chain transfer polymerization.[81] It was filled in styrene-butadiene rubber. The composites showed excellent thermal property (0.45 Wm^{-1} K^{-1}) at mass fraction of 3 %, which was twice higher than that of pure styrene-butadiene rubber. The increase in thermal conductivity was attributed to the synergetic effect of polymer grafted-CNT and reduced GO, strong interface coupling effect between filler and matrix. Zhang *et al.* developed a facile approach that filling silicone rubber with the hybrid of spherical alumina and GNSs.[82] The unique three-dimensional thermally conductive network minimized the thermal contact resistance between fillers and matrix. As a result, a remarkable synergy effect induced high thermal conductivity (3.37 Wm^{-1} K^{-1}), which was 47.1 % higher than that with single additive at the same mass fraction.

The application of graphene in organic phase change materials

Phase change materials (PCMs) change phase or structure by absorbing heat from the surrounding environment to achieve thermal energy storage. PCMs are widely used in aerospace, buildings, refrigeration equipment, communications, electricity and other fields. PCMs can be applied in practice and must possess the following characteristics: (1) huge latent heat capacity; (2) stable thermal properties; (3) high thermal conductivity; (4) non toxicity, non corrosiveness and environmentally friendly; (5) low volume expansion coefficient; (6) inexpensive and

easily available. Organic PCMs like paraffin, fatty acid and polybasic alcohol possess most of the above advantages, but there is a common defect in poor thermal performance. Enhancing thermal conductivity can accelerate the rate of absorbing and releasing heat, thereby increasing the efficiency of heat energy storage systems. In addition, the common methods like filling high thermal conductivity additive and encapsulated PCMs used for improving thermal transport property of organic PCMs. Graphene shows large specific surface area, high thermal conductivity and low density, and thus has become an excellent additive for organic PCMs.

Achieving excellent thermal transport properties for organic PCMs is still a huge challenge. Therefore, there are a great deal of research for improving thermal properties of organic PCMs by adding high thermal conductivity graphene.[83-89] Graphene could greatly reduce defects by high temperature annealing (Figs. 8a 8b 8c).[83] In addition, the thermal conductivity of PCMs filled with annealed graphene (10 wt% loading) was as high as 3.55 $Wm^{-1} K^{-1}$, six times higher than that graphene-based PCMs without annealing, and a 16-fold enhancement than the pristine PCMs (1-octadecanol) (Figs. 8d 8e). Polyethylene glycol/sulfonated based graphene phase change composites were fabricated using a facile solution processing.[85] It is noteworthy that four times enhancement in thermal conductivity (only 4 wt% loading) compared to pure polyethylene glycol. Composite PCMs with different proportion of MWCNT and graphene have been prepared.[89] Results indicated that the composite PCMs showed the most significant synergistic enhancement of heat transfer when the mass ratio of MWCNT : graphene at 3 : 7, with the thermal conductivity increased by 124 %, 55.4 % and 31.8 % compared to pure PCMs, MWCNT-based composite PCMs and graphene-based composite PCMs, respectively.

Encapsulated phase change materials are composed of core and shell using emulsion polymerization, mini-emulsion polymerization, interfacial polymerization or other methods. The PCMs are encapsulated in spherical capsules (Figs. 9a 9b 9c 9d), which can be separated from the external environment and solve the problems of stability, phase separation and corrosion. This unique core-shell structure prolongs the service life of PCMs, and improves the heat transfer efficiency by increasing the contact area of PCMs. A stearic acid based graphene composite microcapsule with core–shell structure was fabricated by latex technology for use as PCMs.[90] The active stearic acid core showed excellent thermal stability and stable structure during phase change. These results make microencapsulated PCMs exhibit great latent heat and high thermal conductivity. A novel PCMs were designed by combination of the microencapsulated n-eicosane with a brookite TiO_2 shell and GNSs. A series of nano-sized titanium dioxide (neicosane@TiO_2) graphene microcapsules were prepared by interfacial polycondensation in emulsion template system.[91] The PCMs were a spherical core−shell structure, where GNSs were attached to the surface of the microcapsules by hydrogen bonding. The phase-change enthalpies of microencapsulated PCMs were over 160 J/g. In addition, the thermal conductivity of PCMs was increased from 0.64 to 0.98 $Wm^{-1} K^{-1}$ in virtue of GNSs with high thermal conductivity.

Conclusions and outlooks

We systematically review the thermal conductivity of graphene and graphene film, as well as the current problems, possible solutions and future directions for graphene in heat transfer enhancement of composite. The composites include nanofluids, thermal conductive polymer materials, organic phase change materials and thermal interface materials. Interface thermal resistance is the key factor affecting the thermal properties of graphene-based composites. Many methods such as directional alignment, functionalization, synergistic enhancement and three-dimensional graphene were used to reduce the interface thermal resistance. However, there are still many problems that remain unsolved, and the future research will mainly focus on the following aspects:

(1) Preparing superstructure materials and constructing high efficient thermal transport channels;

(2) Reducing the interface thermal resistance between graphene and graphene (or matrix), and exploring the mechanism of enhancing heat transfer;

(3) Designing experiments for more accurately measuring the interface thermal resistance.

Conflict of interest

There are no conflicts to declare.

Acknowledgments

The work was supported by National Natural Science Foundation of China (51476094, 51590902), Hunan Provincial Natural Science Fund (2018JJ3478), and the outstanding youth project of Hunan Provincial Education Department (no. 16B236).

References

1. X. Li, W. Cai, J. An, S. Kim, J. Nah, D. Yang, R. Piner and A. Velamakanni, *Science*, 2009, **324(5932)**, 1312-1314.
2. Y. Zhang, Y. W. Tan, H. L. Stormer and P. Kim, *Nature*, 2005, **438(7065)**, 201.
3. C. Lee, X. Wei, J. W. Kysar and J. Hone, *Science*, 2008, **321(5887)**, 385-388.
4. K. S. Novoselov, A. K. Geim, S. Morozov, D. Jiang, M. Katsnelson, I. Grigorieva and A. A. Firsov, *Nature*, 2005, **438(7065)**, 197.
5. C. Yan, J. Wang, W. Kang, M. Cui, X. Wang, C. Y. Foo and P. S. Lee, *Adv. Mater.*, 2014, **26(13)**, 2022-2027.
6. M. F. El-Kady and R. B. Kaner, *Nat. Commun.*, 2013, **4**, 1-9.
7. Z. Sun, J. Zhang, L. Yin, G. Hu, R. Fang, H. M. Cheng and F. Li, *Nat. Commun.*, 2017, **8**, 14627.
8. B. Zhao, D. Chen, X. Xiong, B. Song, R. Hu, Q. Zhang and Y. Chen, *Energy Storage Mater.*, 2017, **7**, 32-39.
9. N. Zhang, M. Q. Yang, S. Liu, Y. Sun and Y. J. Xu, *Chem. Rev.*, 2015, **115(18)**, 10307-10377.
10. C. Han, N. Zhang and Y. J. Xu, *Nano Today*, 2016, **11(3)**, 351-372.
11. K. Q. Lu, X. Xin, N. Zhang, Z. R. Tang and Y. J. Xu, *J. Mater. Chem. A*, 2018, **6(11)**, 4590-4604.
12. Q. Quan, X. Lin, N. Zhang and Y. J. Xu, *Nanoscale*, 2017, **9(7)**, 2398-2416.
13. K. Gaska, R. Kádár, A. Rybak, A. Siwek and S. Gubanski, *Polymers*, 2017, **9(7)**, 294.
14. P. Vecera, J. C. Chacón-Torres, T. Pichler, S. Reich, H. R. Soni, A. Görling and A. Hirsch, *Nat. Commun.*, 2017, **8**, 15192.
15. S. Wan, F. Xu, L. Jiang and Q. Cheng, *Adv. Funct. Mater.*, 2017, **27(10)**, 1605636.
16. Z. Aksamija and I. Knezevic, *Appl. Phys. Lett.*, 2011, **98(14)**, 141919.
17. Z. Guo, D. Zhang and X. G. Gong, *Appl. Phys. Lett.*, 2009, **95(16)**, 163103.
18. W. J. Evans, L. Hu and P. Keblinski, *Appl. Phys. Lett.*, 2010, **96(20)**, 203112.
19. T. Y. Ng, J. J. Yeo and Z. S. Liu, *Carbon*, 2012, **50(13)**, 4887-4893.
20. F. Hao, D. Fang and Z. Xu, *Appl. Phys. Lett.*, 2011, **99(4)**, 041901.
21. S. K. Chien, Y. T. Yang and C. K. Chen, *Appl. Phys. Lett.*, 2011, **98(3)**, 033107.
22. H. Bao, J. Chen, X. K. Gu and B. Y. Cao, *ES Energy Environ.*, 2018, **1**, 16–55.
23. W. Cai, A. L. Moore, Y. Zhu, X. Li, S. Chen, L. Shi and R. S. Ruoff, *Nano Lett.*, 2010, **10(5)**, 1645-1651.
24. H. Xie, L. Chen, W. Yu and B. Wang, *Appl. Phys. Lett.*, 2013, **102(11)**, 111911.
25. W. Jang, Z. Chen, W. Bao, C. N. Lau and C. Dames, *Nano Lett.*, 2010, **10(10)**, 3909-3913.
26. L. Qiu, P. Guo, H. Zou, Y. Feng, X. Zhang, S. Pervaiz and D. Wen, *ES*

Energy Environ., 2018, in press, DOI: 10.30919/esee8c139.
27. T. Schwamb, B. R. Burg, N. C. Schirmer and D. Poulikakos, *Nanotechnology*, 2009, **20(40)**, 405704.
28. X. Fang, L. W. Fan, Q. Ding, X. Wang, X. L. Yao, J. F. Hou and K. F. Cen, *Energy Fuels*, 2013, **27(7)**, 4041-4047.
29. W. Ma, Y. Liu, S. Yan, T. Miao, S. Shi, Z. Xu and C. Gao, *Nano Res.*, 2018, **11(2)**, 741-750.
30. W. Ma, S. Shi and X. Zhang, *J. Vac. Sci. Technol. B*, 2018, **36(2)**, 022903.
31. W. Ma, T. Miao, X. Zhang, K. Takahashi, T. Ikuta, B. Zhang and Z. Ge, *Nanoscale*, 2016, **8(5)**, 2704-2710.
32. D. Ghosh, I. Calizo, D. Teweldebrhan, E. P. Pokatilov, D. L. Nika, A. A. Balandin and C. N. Lau, *Appl. Phys. Lett.*, 2008, **92(15)**, 151911.
33. S. Chen, A. L. Moore, W. Cai, J. W. Suk, J. An, C. Mishra and R. S. Ruoff, *ACS nano*, 2010, **5(1)**, 321-328.
34. J. U. Lee, D. Yoon, H. Kim, S. W. Lee and H. Cheong, *Phys. Rev. B*, 2011, **83(8)**, 081419.
35. S. Chen, Q. Wu, C. Mishra, J. Kang, H. Zhang, K. Cho and R. S. Ruoff, *Nat. Mater.*, 2012, **11(3)**, 203.
36. S. Ghosh, W. Bao, D. L. Nika, S. Subrina, E. P. Pokatilov, C. N. Lau and A. A. Balandin, *Nat. Mater.*, 2010, **9(7)**, 555.
37. X. Xu, L. F. Pereira, Y. Wang, J. Wu, K. Zhang, X. Zhao, B. H. Hong, *Nat. Commun.*, 2014, **5**, 3689.
38. W. Yu, G. Liu, J. Wang, X. Huang, H. Xie and X. Wang, *Synth. React. Inorg. Met.-Org. Chem.,* 2013, **43(9)**, 1197-1205.
39. W. Yu, H. Xie, F. Li, J. Zhao and Z. Zhang, *Appl. Phys. Lett.*, 2013, **103(14)**, 141913.
40. N. J. Song, C. M. Chen, C. Lu, Z. Liu, Q. Q. Kong and R. Cai, *J. Mater. Chem. A*, 2014, **2(39),** 16563-16568.
41. P. Kumar, F. Shahzad, S. Yu, S. M. Hong, Y. H. Kim and C. M. Koo, *Carbon*, 2015, **94**, 494-500.
42. N. Wang, M. K. Samani, H. Li, L. Dong, Z. Zhang, P. Su and X. Xu, *Small*, 2018: 1801346.
43. B. Shen, W. Zhai and W. Zheng, *Adv. Funct. Mater.*, 2014, **24(28)**, 4542-4548.
44. E. Sadeghinezhad, M. Mehrali, R. Saidur, M. Mehrali, S. T. Latibari, A. R. Akhiani and H. S. C. Metselaar, *Energy Convers. Manage.*, 2016, **111**, 466-487.
45. W. Yu, H. Xie and W. Chen, *J. Appl. Phys.*, 2010, **107(9)**, 094317.
46. H. Yarmand, S. Gharehkhani, G. Ahmadi, S. F. S. Shirazi, S. Baradaran, E. Montazer and M. Dahari, *Energy Convers. Manage.*, 2015, **100**, 419-428.
47. T. T. Baby and S. Ramaprabhu, *J. Appl. Phys.*, 2010, **108(12)**, 124308.
48. M. Kole and T. K. Dey, *J. Appl. Phys.*, 2013, **113(8)**, 084307.
49. A. Ghozatloo, M. Shariaty-Niasar and A. M. Rashidi, *Int. Commun. Heat Mass Transfer*, 2013, **42**, 89-94.
50. M. R Esfahani, E. M. Languri and M. R. Nunna, *Int. Commun. Heat Mass Transfer*, 2016, **76**, 308-315.
51. T. T. Baby and S. Ramaprabhu, *Nanoscale Res. Lett.*, 2011, **6(1)**, 289.
52. T. T. Baby and R. Sundara, *J. Phys. Chem. C*, 2011, **115(17)**, 8527-8533.
53. C. Hermida-Merino, M. Pérez-Rodríguez, A. B. Pereiro, M. M. Piñeiro and M. J. Pastoriza-Gallego, *ACS Omega*, 2018, **3(1)**, 744-752.
54. A. Naddaf and S. Z. Heris, *Int. Commun. Heat Mass Transfer*, 2018, **95**, 116-122.
55. W. Yu, H. Xie, X. Wang and X. Wang, *Phys. Lett. A*, 2011, **375(10)**, 1323-1328.
56. X. Li, Y. Chen, S. Mo, L. Jia and X. Shao, *Thermochim. Acta*, 2014, **595**, 6-10.
57. S. S. J. Aravind and S. Ramaprabhu, *Rsc Adv.*, 2013, **3(13)**, 4199-4206.
58. W. Yu, C. Liu, L. Qiu, P. Zhang, W. Ma, Y. Yue, H. Xie and L. Larkin, *Eng. Sci.*, 2018, **2**, 95–97.
59. C. Liu, M. Chen, D. Zhou and D. Wu, W. Yu, *J. Nanomater*. 2017, 2017.
60. C. Liu and G. Hu, *Appl. Therm. Eng.*, 2015, **90**, 193-198.
61. P. Zhang, J. Zeng, S. Zhai, Y. Xian, D. Yang and Q. Li, *Macromol. Mater. Eng.*, 2017, **302(9)**, 1700068.
62. T. Cui, Q. Li, Y. Xuan and P. Zhang, *Microelectronics Reliability*, 2015, **55(12)**, 2569-2574.
63. L. Zhao, H. Liu, X. Chen, S. Chu, H. Liu, Z. Lin and H. Zhang, *J. Phys. Chem. C*, 2018, **6(39)**, 10611-10617.
64. K. M. Razeeb, E. Dalton, G. L. W. Cross and A. J. Robinson, *Int. Mater. Rev.*, 2018, **63(1)**, 1-21.
65. P. Zhang, P. Yuan, X. Jiang, S. Zhai, J. Zeng, Y. Xian and D. Yang, *Small*, 2018, **14(2)**, 1702769.
66. Y. Guo, G. Xu, X. Yang, K. Ruan, T. Ma, Q. Zhang and Z. Guo, *J. Phys. Chem. C*, 2018, **6(12)**, 3004-3015.
67. J. Gu, C. Liang, X. Zhao, B. Gan, H. Qiu, Y. Guo and D. Y. Wang, *Compos. Sci. Technol.*, 2017, **139**, 83-89.
68. H. Yan, Y. Tang, W. Long and Y. Li, *J. Mater. Sci.*, 2014, **49(15)**, 5256-5264.
69. J. Renteria, S. Legedza, R. Salgado, M. P. Balandin, S. Ramirez, M. Saadah and A. A. Balandin, *Mater. Des.*, 2015, **88**, 214-221.
70. C. C. Teng, C. C. M. Ma, C. H. Lu, S. Y. Yang, S. H. Lee, M. C. Hsiao and T. M. Lee, *Carbon*, 2011, **49(15)**, 5107-5116.
71. Y. Wang, H. F. Zhan, Y. Xiang, C. Yang, C. M. Wang and Y. Y. Zhang, *J. Phys. Chem. C*, 2015, **119(22)**, 12731-12738.
72. X. Shen, Z. Wang, Y. Wu, X. Liu and J. K. Kim, *Carbon*, 2016, **108**, 412-422.
73. S. Y. Yang, W. N. Lin, Y. L. Huang, H. W. Tien, J. Y. Wang, C. C. M. Ma and Y. S. Wang, *Carbon*, 2011, **49(3)**, 793-803.
74. A. Yu, P. Ramesh, X. Sun, E. Bekyarova, M. E. Itkis and R. C. Haddon, *Adv. Mater.*, 2008, **20(24)**, 4740-4744.
75. W. Yu, H. Xie and L. Chen, *J. Eng. Thermophys.*, 2013, **34(9)**, 1749-1751.
76. B. Yin, J. Wang, H. Jia, J. He, X. Zhang and Z. Xu, *J. Mater. Sci.*, 2016, **51(12)**, 5724-5737.
77. J. Song, C. Chen and Y. Zhang, *Compos. Part A*, 2018, **105**, 1-8.
78. Z. Liu, H. Zhang, S. Song and Y. Zhang, *Compos. Sci. Technol*., 2017, **150**, 174-180.
79. W. Yu, H. Xie, L. Yin, J. Zhao, L. Xia and L. Chen, *Int. J. Therm. Sci.*, 2015, **91**, 76-82.
80. X. Huang, C. Zhi and P. Jiang, *J. Phys. Chem. C*, 2012, **116(44)**, 23812-23820.
81. S. Song and Y. Zhang, *Carbon*, 2017, **123**, 158-167.
82. Y. Zhang, W. Yu, L. Zhang, J. Yin, J. Wang and H. Xie, *J. Thermal Sci. Eng. Appl.*, 2018, **10(1)**, 011014.
83. G. Xin, H. Sun, S. M. Scott, T. Yao, F. Lu, D. Shao and J. Lian, *ACS Appl. Mater. Interfaces*, 2014, **6(17)**, 15262-15271.
84. J. Yang, X. Li, S. Han, Y. Zhang, P. Min, N. Koratkar and Z. Z. Yu, *J. Mater. Chem. A*, 2016, **4(46)**, 18067-18074.
85. H. Li, M. Jiang, Q. Li, D. Li, Z. Chen, W. Hu and C. Xiong, *Energy Convers. Manage.*, 2013, **75**, 482-487.
86. F. Yavari, H. R. Fard, K. Pashayi, M. A. Rafiee, A. Zamiri, Z. Yu and N. Koratkar, *J. Phys. Chem. C*, 2011, **115(17)**, 8753-8758.
87. S. Harish, D. Orejon, Y. Takata and M. Kohno, *Appl. Therm. Eng.*, 2015, **80**, 205-211.
88. H. Babaei, P. Keblinski and J. M. Khodadadi, *Int. J. Heat Mass Tran.*, 2013, **58(1-2)**, 209-216.
89. D. Zou, X. Ma, X. Liu, P. Zheng and Y. Hu, *Int. J. Heat Mass Tran.*, 2018, **120**, 33-41.
90. H. Liu, X. Wang and D. Wu, *ACS Sustain. Chem. Eng.*, 2017, **5(6)**, 4906-4915.
91. T. D. Dao and H. M. Jeong, *Sol. Energy Mater. Sol. Cells*, 2015, **137**, 227-234.